Review Article

Progress in Biological Sciences

Vol. 4, Number 2, Summer / Autumn 2014/133-152

Demystifying EPR: A Rookie Guide to the Application of Electron Paramagnetic Resonance Spectroscopy on Biomolecules

Received: June 15, 2014; Accepted: September 30, 2014

Yaser NejatyJahromy*, Erik Schubert

Institute of Physical and Theoretical Chemistry, University of Bonn, Wegelerstr. 12, 53115, Bonn, Germany

ABSTRACT

Electron Paramagnetic Resonance (EPR) spectroscopy, also known as Electron Spin Resonance (ESR) especially among physicists, is a strong and versatile spectroscopic method for investigation of paramagnetic systems, i.e. systems like free radicals and most transition metal ions, which have unpaired electrons. The sensitivity and selectivity of EPR are notable and intriguing as compared to other spectroscopic methods and approaches. As a qualitative method, EPR can detect species down to the nanomolar range. On the other hand, the specificity of the method stems from spectral features which directly depend on the types, distances, and relative orientations of the atoms in the neighborhood of the electron spin centers. In addition to structural information, EPR can be used to elucidate time dependent behavior of the studied system and it is applicable to systems of different size, ranging from small molecules to macromolecules. The following short review of general EPR methods is intended for an audience with little prior knowledge about EPR. It includes examples of suitable representative systems, techniques for the study of short lived paramagnetic species and even diamagnetic molecules, and introduces the reader to tools necessary for making sense of the spectra. This paper focuses only on *continuous wave* (*cw*) EPR and does not elaborate on the more advanced *pulsed* EPR methods.

Keywords: EPR spectroscopy, hyperfine, paramagnetic, radical, spin label.

* **Corresponding author:** nejaty@pc.uni-bonn.de

Introduction

Unpaired electrons play a pivotal role in biology. The first top-level class of enzymes out of six, oxidoreductases (EC 1), catalyze the transfer of electrons from one molecule to another (1). Since electrons are typically transferred in a one-at-a-time fashion, the reactions of this class of enzymes involve species with unpaired electrons, i.e. paramagnetic species, at some point through the course of their catalysis. Some reactions of this class are at the core of fundamental biochemical processes such as photosynthesis, nitrogen fixation and cellular respiration. Often times, cofactors serve as the provider, acceptor or transient accommodator of the transferred electron while switching between paramagnetic and diamagnetic states. Such cofactors can be organic (e.g. flavin coenzymes) or inorganic metal containing species. In fact, oxidoreductases and metalloproteins account for close to half of all proteins (2, 3).

Understanding Basic Spectra

Imagine a scenario under which the researcher is following the dissociation of an electron from tyrosine 122 of *E. coli* ribonucleotide reductase and its oxidation into a tyrosine radical (4). Understanding the spectroscopy of such unpaired electrons requires the recognition of the factors which affect its energy and energy levels. So, in the following paragraphs, we discuss the terms contributing to the Hamiltonian (i.e. the energy) of the unpaired electron. For the simple system of one unpaired electron (S = ½) and a single nucleus with I = ½, the energy of the system is the result of the interaction of the unpaired electron with the external field, the mutual influence of the electron and the nucleus, and the effect of the external field on the nucleus, with the last two items being typically of the same order of magnitude.

EPR owes its existence to the magnetic moment of the unpaired electron, which is another way of saying that in the context of EPR an unpaired electron can be thought of as a "quantum magnet". Although classical physics analogies do not hold thoroughly in the world of atoms, they are often helpful in getting an insight and developing the starting intuition, and thus, we use them here. The magnetic moment of the unpaired electron interacts with the externally applied magnetic field in a similar fashion that a compass interacts with the earth's magnetic field. This effect is called *electronic Zeeman interaction* which typically constitutes one of the largest contributions to the Hamiltonian of the unpaired electron and it is denoted as

$$\mathbf{H}_{EZI} = \beta_e \boldsymbol{B}_0^T \hat{\boldsymbol{g}} \boldsymbol{S}$$

where β_e is the Bohr magneton (a physical constant), $\boldsymbol{B}_0^T$ is the external magnetic field (transposed), $\hat{\boldsymbol{g}}$ is the g tensor (i.e. a 3×3 matrix, marked by the caret symbol) and $\boldsymbol{S}$ is the electron spin operator whose values reflect the spin state of the electron.

If we were to study a free electron unbound in any molecule, all three principal values of the g tensor would be g_e = 2.002319. However, these three principal values do deviate from this number due to the residence of the electron in a molecule (which results in the so called *spin-orbit coupling*) and indeed carry valuable information on the electronic state, the bonding and the geometry of the molecule. The g tensor can be either isotropic, with its three principal values more or less the same ($g_x \approx g_y \approx g_z$), axial, with only two equal principal values ($g_x \approx g_y = g_{||}$ and $g_z \approx g_\perp$), or orthorhombic, with three different principal values ($g_x \neq g_y \neq g_z$). When

species with the anisotropic paramagnetic parameters are investigated in solution, where the fast rotation averages out the anisotropic effects, only the mean values are observed. That is, for a g tensor, $g_{\text{observed}} = \frac{1}{3}\left(g_x + g_y + g_z\right)$. In frozen samples, due to lack of motion, anisotropies are preserved and detected. For instance, axial and orthorhombic g tensors would lead to peaks which are spread over the whole span of g, known as powder patterns or Pake patterns (5).

In a similar fashion to *electronic Zeeman interaction* discussed above, the nuclei with a magnetic moment also interact with the external magnetic field. This effect, namely *nuclear Zeeman interaction*, is much smaller than its electronic counterpart; however, this term and other small terms of the EPR Hamiltonian cannot be ignored. The contribution of the *nuclear Zeeman interaction* is:

$$\mathbf{H}_{NZI} = -\sum_k \beta_n g_{n,k} \boldsymbol{B}_0^T \boldsymbol{I}_k$$

where, similar to the case of the electron, β_n is the nuclear magneton, $g_{n,k}$ is the nuclear g factor for atom k, $\boldsymbol{B}_0^T$ is the external magnetic field (transposed), $\boldsymbol{I}_k$ is the nuclear spin operator, and the summation is on all the nuclei, but only nuclei with a nuclear spin ($I \geq$ ½) contribute. β_e and β_n are the natural units of electron and nuclear magnetic dipole moments respectively. Since $\frac{\beta_e}{\beta_n} = \frac{m_n}{m_e}$, the electron Zeeman effect is two or three orders of magnitude larger than the nuclear Zeeman effect. This is the principle behind the high sensitivity of EPR and why EPR spectroscopists can get away with micromolar protein solutions while their NMR colleagues typically need millimolar concentrations. Since solubility is not an issue and only an electron spin as well as a few of its neighboring nuclear spins are detected (and thus the spectrum is not that crowded), unlike NMR, the protein size restriction is virtually lifted in EPR.

Nuclei affect the energy of the system in two other ways. First, similar to the case of two bar magnets, the electron spin and a nuclear spin interact. The resulting term in the Hamiltonian is called *hyperfine interaction*; it depends on both the distance and the relative orientation of the two spins and makes EPR the superb tool of choice, for instance, for determination of the presence, the distance and the orientation of a ligand. Secondly, each nucleus with $I >$ ½ possesses what is called a *nuclear quadrupole interaction* between the non-spherically distributed nuclear charge and the local electric field gradient.

$$\mathbf{H}_{HFI} + \mathbf{H}_{NQI} = h\sum_k \boldsymbol{S}^T \widehat{\boldsymbol{A}}_k \boldsymbol{I}_k + h\sum_{\boldsymbol{k}, \boldsymbol{I_k} > \frac{1}{2}} \boldsymbol{I}_k^T \widehat{\boldsymbol{P}}_k \boldsymbol{I}_k$$

Here, $\widehat{\boldsymbol{A}}_k$ and $\widehat{\boldsymbol{P}}_k$ are the individual hyperfine and the quadrupole tensors. The aforementioned four terms make up the Hamiltonian of the system with a single electron spin of ½:

$$\mathbf{H}_{total\,(S=\frac{1}{2})} = \mathbf{H}_{EZI} + \mathbf{H}_{NZI} + \mathbf{H}_{HFI} + \mathbf{H}_{NQI}$$

Having this knowledge of EPR Hamiltonian, it is now time to relate it to a spectrum. Figure 1 shows the energy diagram of a system of an electron spin of S = ½ and a single nucleus of I =1, where the hyperfine coupling constant is positive and much larger than the nuclear Larmor frequency and the quadrupole interaction is ignored. A real life example of such a system is any of the widely used nitroxide-based spin labels (see the section on spin labels below).

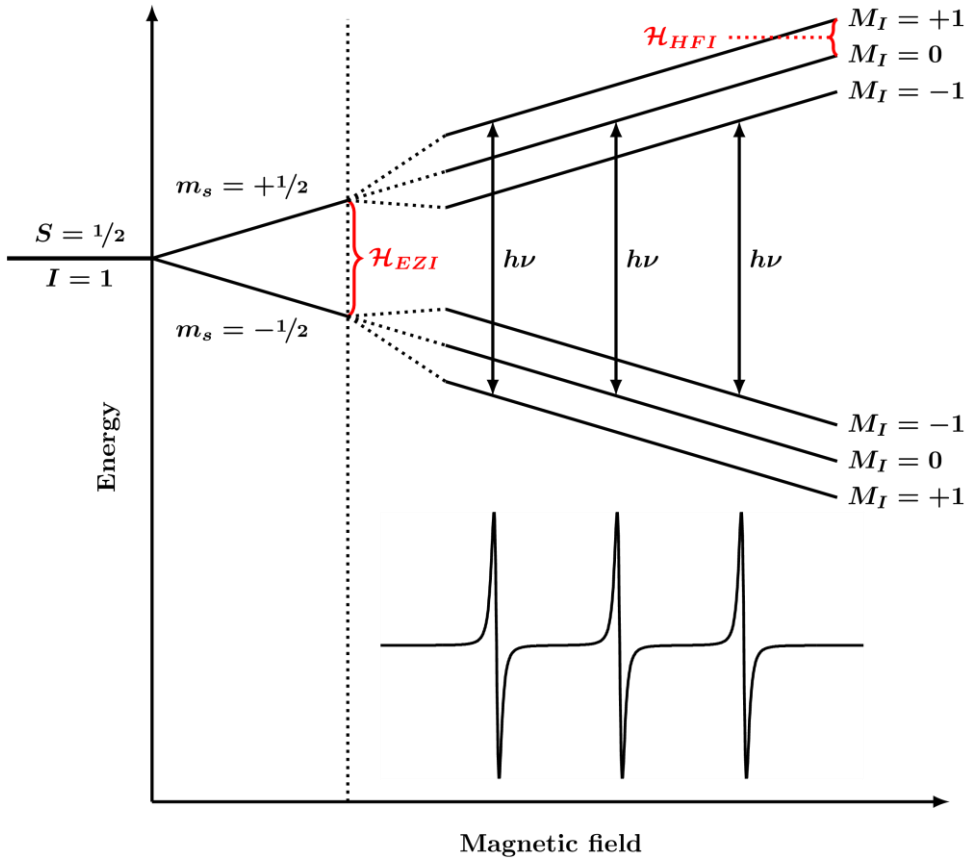

Figure 1. Energy scheme of EPR transitions for a system with one unpaired electron coupled (*s*= ½) to a nucleus with *I* = 1 such as the nitrogen atom of a nitroxidespin label and the expected room temperature *cw* EPR spectrum in arbitrary units. The diagram isvalid for the case of $\frac{A}{2} \gg \nu_I$.

In the absence of an externally applied magnetic field, all orientations of magnetic moments of the electron have the same energy. Upon applying the external field, electron spins will assume two orientations, parallel or anti-parallel to the field, with two different associated energies. As mentioned above, this energy split, $\mathbf{H}_{EZI}$, is field dependent. These two energy levels are further split by the (field independent) interaction of the electron magnetic moment and the nuclear magnetic moment of the nitrogen atom. In the regular (i.e. perpendicular mode) *cw* EPR experiment, the selection rules of $\Delta m_s = 1$ and $\Delta m_I = 0$ apply. When the incident microwave matches the energy gap of the three allowed transitions, an "absorption" happens, which can manifest itself in any of the three peaks.

Note that when $S > ½$, there exists a *zero-field interaction* denoted by tensor $\hat{\boldsymbol{D}}$ which as the name suggests, is field independent ($\mathbf{H}_{ZFI} = \boldsymbol{S}^T\hat{\boldsymbol{D}}\boldsymbol{S}$). Moreover, for the case when two (or more) electron spins are present, both exchange and dipolar interactions of the electrons (summarized in a single tensor, $\hat{\boldsymbol{J}}$) should be considered as well ($\mathbf{H}_{EEI} = \boldsymbol{S}_1^T\hat{\boldsymbol{J}}\boldsymbol{S}_2$).

Instrumentally, EPR experiments can be divided into two groups: *continuous wave* (*cw*) methods and *pulsed* techniques. An example often given to elucidate the different approach in *cw* versus *pulsed* methods is two ways of tuning a musical instrument. Similar to *cw* EPR, one can have a variable frequency

generator and scan the whole frequency range to find out which frequencies are absorbed by the instrument. Alternatively, one can give a sudden impulse to simultaneously excite virtually all vibration modes and follow the emission as a function of time. This "time trace" can then be Fourier transformed to obtain the absorption/emission frequencies.

cw EPR was developed first and is instrumentally less demanding. The authors maintain that the introduction of more recent *pulsed*-capable instruments and methods overshadows, at least partially, the versatilities and usefulness of *cw* EPR. Furthermore, *cw* EPR is more widely available, *pulsed* EPR samples are usually checked for quality beforehand with *cw* EPR, and *cw* EPR is the standard gateway of newcomers to the world of EPR. The current review thus covers only *cw* EPR techniques and *pulsed* methods will hopefully be covered in a future issue.

Continuous Wave EPR Methods and Practices

RT vs low T

For solutions, EPR spectroscopy can be performed both on liquid samples and/or frozen ones. The choice here affects the amount of information gained and the difficulty of data analysis. Additionally, the range of temperatures usually used in EPR spans from < 3 K to > 300 K. While "organic" radicals are usually studied over liquid nitrogen accessible range (> 77 K), often times EPR of metal containing radicals require a lower temperature even when the metal center is only in the vicinity of an organic radical and not the studied paramagnetic center itself. A few parameters which influence the determination of the optimal temperature and the phase of the medium for data acquisition are considered here.

Relaxation

At room temperature, solution EPR is generally limited to radicals with a light-atom spin center such as organic radicals and isolated non-metallic cofactors. This is not the case for Nuclear Magnetic Resonance (NMR), another magnetic resonance spectroscopic method. Roughly speaking, *relaxation time* reflects the time it takes for an excited spin to get back to the ground state and is inversely related to the line widths on the spectrum. While typical relaxation times in NMR are in the millisecond to second range, characteristic lifetimes of the spin states in EPR are in the microsecond to nanosecond range under experimental conditions. This is why in nuclear-spin-based magnetic resonance imaging (MRI) one sometimes tries to reduce the relaxation times (e.g. by using relaxing agents (6)), whereas for performing EPR on a typical metal containing protein one may need to go to liquid helium temperatures to sufficiently increase the relaxation time of electron spins (7). For such a fast relaxing paramagnetic center, the spectrum is too broad to be detected at all at higher temperatures.

Power saturation

Despite what may come to mind after reading the last section on relaxation, faster relaxation is not always unfavorable and a low relaxation rate is an issue to be dealt with in some instances. A net absorption of microwave (i.e. EPR signal) depends on a population difference between the lower and higher energy levels. If the incident power is greater than the dissipated power through relaxation, the Boltzmann equilibrium is perturbed toward a diminished population

difference which results in a smaller signal. This phenomenon is called saturation. Under non-saturating conditions, the signal intensity is proportional to the square root of microwave power. Upon (partial) saturation, the signal does not grow accordingly and if the power is increased further, the signal eventually disappears. Saturation mainly comes into the picture for organic radicals for which the *g* tensor is typically quite isotropic and relaxation is slow. While for qualitative measurements and the study of spectral features partial saturation is not necessarily harmful, quantitative measurements are always done under non-saturating conditions (see the section on quantification below).

Flat cell

EPR spectroscopy relies on the interaction of the spin-caused magnetic moment of unpaired electrons with the magnetic component of electromagnetic waves of microwave range. However, from the kitchen microwave oven, one knows that water molecules absorb electromagnetic waves of such frequencies since its very large dipole moment strongly interacts with electrical field (dielectric constant of water, $k(H_2O)$, is 80). This absorption makes EPR impossible for aqueous solution in regular EPR tubes. However, there is an easy fix for this issue and flat cells were developed to address this problem (8). A flat cell is a thin EPR "cuvette" whose virtually 2-dimentional nature makes it possible to orient the sample along the electrical nodal plane of the resonator (TE_{102}) and, therefore, the solvent does not experience the electrical field and no absorption occurs. For (liquid) solvents with relatively small dielectric constants such as a lot of common organic solvents, the interaction with the electrical field is limited and regular sample tubes are sufficient. In addition, upon freezing, the dielectric constant of water drops significantly, making the electrical field interaction a non-issue.

Spin labels: Studying Diamagnetic Molecules

Is EPR to be deemed useless when the system to be studied is not inherently paramagnetic? The short answer is "absolutely not". Similar to fluorescence spectroscopic techniques in which a green fluorescent protein (GFP) or the like is engineered into the targeted molecule, a paramagnetic adduct can be made from the diamagnetic molecule of interest and any member of the large library of spin labels. Structurally speaking and in contrast to the case of GFP, spin labels are typically non-invasive due to their small size. Most spin labels are nitroxide based, with the functional group $R_2N–O•$ in which R is hydrocarbon chain/cycle. One of the most extensively used spin labels is MTSSL (*S*-(2,2,5,5-tetramethyl-2,5-dihydro-1H-pyrrol-3-yl)methyl methanesulfonothioate) which covalently attaches to proteins via cysteine residues through a disulfide bond (Fig. 1, Fig. 2). An alternative and emerging spin label class is of those based on trityl radicals (9).

Spin labels can be used to paramagnetically label proteins (10), nucleic acids (11) and lipids (12). The general methods can be tailored to cover a broad range of applications. For instance, to preserve the functionally important cysteine residues, unnatural amino acids such as *p*-acetyl-L-phenylalanine (*p*-AcPhe) can be expressed and later reacted with appropriate reagents to generate a nitroxide side chain (13).

Chemical attachment of a spin label is not the only way to go. It is sometimes possible to add a spin label to a location non-covalently. For instance, a rigid spin-labelled

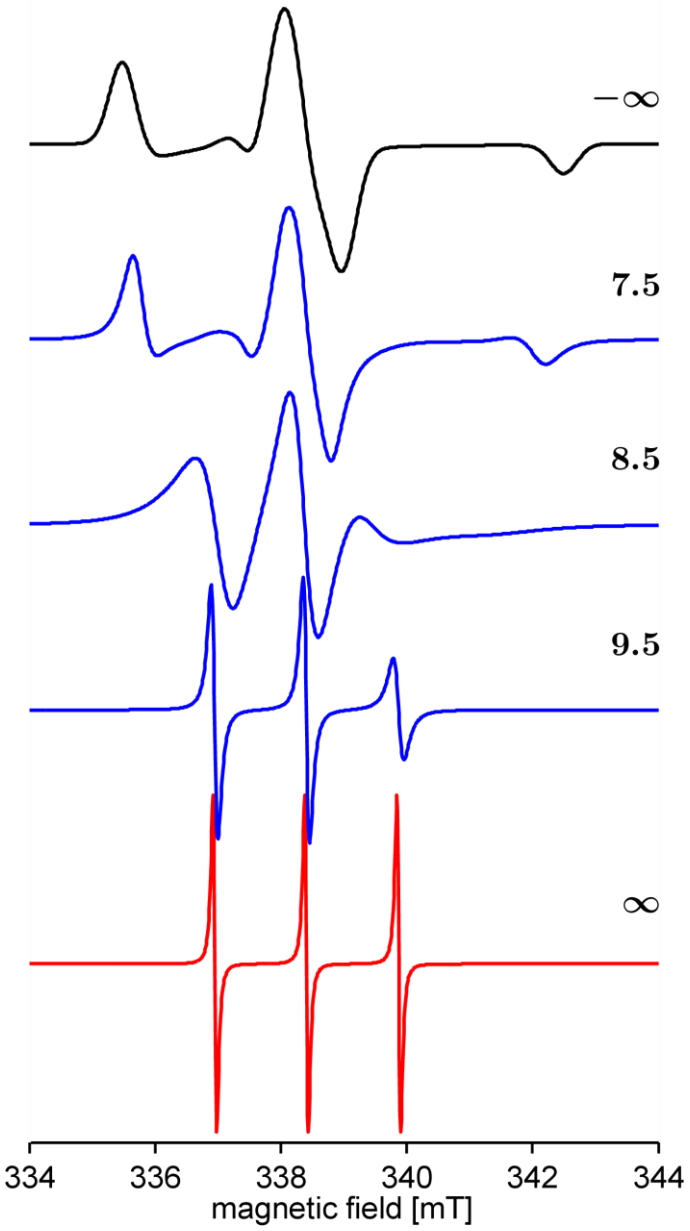

Figure 2. Probing the dynamics of a spin center with EPR. Simulated *cw* EPR spectrum of a nitroxide spin label (at X-band) is drastically affected by the correlation time of its motion.The number on each spectrum is the opposite of the logarithm of the characteristic correlation time (in seconds) used for each case.∞ and–∞ indicate the fast motion (non-viscous liquid solution) and rigid (frozen solution) limits respectively.

cysteine analogue has been used to label double-stranded DNA (14). Spin labels can also be *virtually* attached to one's protein of choice, i.e. prior to site directed mutagenesis and labeling, software tools such as mtsslWizard can be used for *in silico* spin labeling to gain insight into their expected mobility and solvent exposure (15).

Trapping: Dealing with unstable and/or transient radicals

One of the methods which can be used for EPR detection of some short-lived radicals is spin-trapping (8, 16, 17). Spin traps are small diamagnetic organic molecules which react with the unstable radical to generate a more stable radical adduct. They can be used to

quantitatively measure the amount of the short-lived species. The technique can also sometimes be used to differentiate between two possible original paramagnetic species. Figure 3 shows how the widely used spin trap 5,5-Dimethyl-1-Pyrroline-N-Oxidethe (DMPO) distinguishes two biologically relevant O-centered radicals, namely superoxide and hydroxyl radicals (18, 19). Similarly, C-, N- and S-centered radicals could be investigated (20) and in fact libraries of parameters for a large range of adducts are available (21).

A more general approach to the radical instability issue is rapid freeze quenching (RFQ). While spin trapping is particularly helpful with unstable radicals at low concentrations, freeze quenching can trap an unstable/transient radical at virtually any point of the reaction course (22, 23). An RFQ setup is typically comprised of a mixing system capable of performance at multiple predetermined constant flow rates and a freezing unit (22). The freezing is usually made possible through liquid nitrogen cooled liquids (e.g. isopentane) or metal surfaces and wheels (22). Figure 1 of supplemental information shows how RFQ can be utilized to study the kinetics of the transition of high-spin ferric heme ($S = \frac{5}{2}$) to low-spin heme ($S = \frac{1}{2}$) in myoglobin, a reaction typically done to "calibrate" one's RFQ setup. RFQ has been and still is a fundamental method in the preparation of EPR-suitable samples of some of the most sophisticated electron transfer biochemical reactions (24-26).

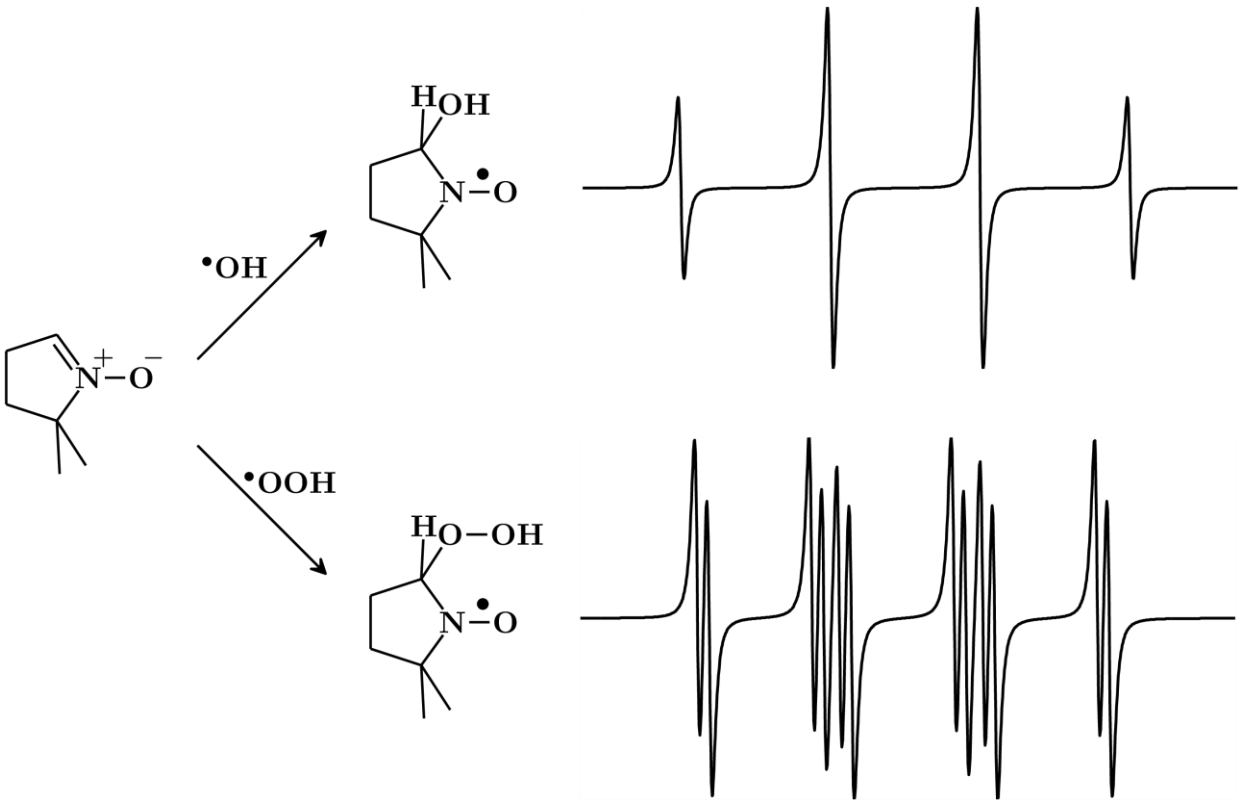

Figure 3. The spin trap DMPO can react with unstable superoxide and hydroxyl radicals to help in their detection and/or identification.

Isotope substitution

Spin centers are often in the core or in the vicinity of reaction centers. When EPR is being used to probe the electronic structure and the geometry of such a center, an isotope substitution is performed such that the reporter atom is changed without affecting the biochemistry. Often times, interpretation of a spectrum are hindered by the large number of paramagnetic parameters such as hyperfine coupling constants of all of the involved atoms. Upon an isotope swap, the hyperfine constant of the new isotope is equal to the corresponding value of the initial isotope scaled with the ratio the nuclear g factors, g_n, of the two isotopes. So by performing EPR on isotopologues, the number of variables for the simulation (and thus the interpretation) of the spectrum does not change while the number of constraints is increased by the new data set, which in turn makes the simulation easier. Specifically, when naturally abundant hydrogen (99.99% ${}^{1}_{1}\mathrm{H}$) is substituted with ${}^{2}_{1}\mathrm{H}$ (deuterium), the corresponding hyperfine couplings are scaled down by a factor of $\frac{g_n({}^{1}_{1}\mathrm{H})}{g_n({}^{2}_{1}\mathrm{H})} \approx 6.5$ which in some cases effectively removes the contributions of hydrogen atoms to the *cw* spectrum. For a ${}^{14}_{7}\mathrm{N}$ to ${}^{15}_{7}\mathrm{N}$ substitution, the change in the hyperfine couplings is not as drastic, but the number of spectral peaks does diminish due to the difference in the nuclear spin number (I (${}^{14}_{7}\mathrm{N}$) =½, I (${}^{15}_{7}\mathrm{N}$) =1). Electron spin population on a spinless oxygen atom (I (${}^{16}_{8}\mathrm{O}$) =0) is not directly "reported" unless it is substituted by ${}^{17}_{8}\mathrm{O}$, with I=$\frac{5}{2}$. Specific isotope labeling can be used to single out the contribution of the particular atom to the spectrum. This method was used to show that among the five nitrogens of the cofactor tetrahydrobiopterin cation radical in nitric oxide synthase, nitrogen 5 has the highest share of the electron spin (7).

If the electron spin density is too small on a locus, due to distance or lack of bonding for instance, no change is observed upon isotope labeling of that spot. This observation was used in the identification of the radical intermediate in tyrosine scission to the CO and CN^- ligands of [FeFe] Hydrogenase (24).

Making sense of the experimental spectra

Complexity of spectra increases rapidly with the number of atoms. Even with a small number of atoms, quite a few paramagnetic parameters contribute to the overall shape and features of an anisotropic spectrum. Six parameters (3 principal values and 3 Euler angles) are necessary to describe any of the involved tensors, be it the g tensor or any of the hyperfine tensors or the like. As a result, the spectra are often too complex to determine the paramagnetic parameters directly, e.g. by measuring a peak to peak splitting. Fortunately, computational tools have been developed to "extract" the desired parameters.

Simulations

Knowledge of the parameters contributing to the energy of the unpaired electron (i.e. its Hamiltonian), allows simulation of the spectrum. The Hamiltonian leads to the energy levels, from which the energy/frequency of each transition and hence the location of each peak can be deduced. Simulation of an EPR spectrum serves two purposes. Prior to an experiment, provided that some estimation of the paramagnetic parameters are available (see below), the spectrum can be constructed *in silico* to see what can be expected. Secondly and more importantly, the "real" (experimental) paramagnetic parameters can be approximated

by finding the parameters which yield the best fit to the acquired spectrum. One such EPR simulation software is *EasySpin* (27), which runs as an added toolbox to the numerical computation package MATLAB®. *EasySpin* is capable of simulating (and fitting) a wide range of EPR spectra and is available free of charge. The reader is highly encouraged to try to virtually acquire some EPR spectra using this toolbox. All the simulations in this paper are done using *EasySpin*; the corresponding MATLAB codes are made available to the reader in the supplemental materials which can be visualized after downloading and installation of the *EasySpin* toolbox in MATLAB. Other available software, to name just a few, are Xsophe (28), XEMR (29), EPR-NMR (30).

DFT

Often times, a "close enough" guess of the paramagnetic parameters is necessary or at least helpful to start the simulation/fitting of a spectrum. Such guesses may come from previous studies on similar compounds. But occasionally, no such previous work is available. A more general approach is the employment of quantum chemistry computational packages. Such packages typically use *ab initio* or semi-empirical methods to calculate the wave function and/or electron density of the many-atom system. The resulting information can further be used to predict paramagnetic parameters such as the *g* tensor and the *A* tensors. The prediction step is normally preceded by a geometry optimization step due to the fact that paramagnetic parameters are very sensitive to the atom-atom distances and angles. One of such packages is ORCA (31), which is available free of charge. The *eprnmr* module in ORCA is to be utilized to predict the paramagnetic parameters. The same can be done by the quantum chemistry program *Gaussian*® using the *nmr* keyword. A sample output file of EPR parameter prediction using ORCA for the nitroxide molecule TEMPO is available in the supplemental materials. To help with the visualization of the ORCA calculated tensors and their orientations with respect to the molecular frame, we developed a MATLAB function called *ORCAview*, also included as a supplementary material, that the reader may find useful. The ORCA predicted tensors can be read by *ORCAview* and can further be used to simulate a spectrum (see supplemental materials).

EPR in action

To highlight the potential and versatility of EPR in the study of biochemical systems, a few examples are given below.

Distance measurement

cw EPR can be used as a nm range ruler for measuring distances in biomolecules. Dipolar-dipolar interaction between any two spins has an r^{-3} dependency which can be used for this purpose. Such dipolar interactions are present in the hyperfine effects, where the nuclear spins interact with the electron spins, and they can be used for the measurement of the electron-nucleus of short (< 10 Å) and particularly, very short (< 5 Å) distance ranges (32 , 33). However, in the context of distance measurement in EPR, what is meant is usually dipolar interactions between two paramagnetic centers (i.e. two electron spins). The physical distance between two sites in a protein, DNA, RNA and/or lipid molecules can be estimated accurately both intra- and inter-molecularly; engineering two nitroxide spin labels into the intended loci is the most typical approach. Multiple distance constraints resulting from performing more than one such measurements

can help determine tertiary and quaternary structural models of biomolecules as well as structural changes (34-38). *cw* EPR is a strong tool in the determination of small (5–10 Å) and intermediate (10–20 Å) inter-spin distances, and larger inter-electron distances (up to ca. 20 Å) can be covered by using perdeuterated nitroxide spin probes (38-40). These small and intermediate ranges are not typically accessible to *pulsed* EPR methods for distance measurement like PELDOR. However, appropriate *pulsed* EPR methods such as PELDOR can be used to extend the upper limit to ca. 80 Å (41, 42).

Quantification and binding constants

cw EPR is a quantitative technique, i.e. the signal intensity is proportional to the number of spins present in the sample. The main factor to consider in using EPR for quantification is that such experiments need to be performed under non-saturating conditions (see sections on relaxation and power saturation above). Under non-saturation, the EPR signal is proportional to the magnetic field (B) component of the incident microwave which itself grows with the square root of the microwave power. So if the power is increased by a factor of 4 (a power attenuation decrease by 6 dB), the signal intensity should be doubled (43). If the signal behavior is different, then the EPR signal is being saturated, i.e. the relaxation rate of hot spins is not fast enough to compete with the microwave excitation, and lower microwave should be tried until one reaches the non-saturation regime. Correlation between the signal intensity and the actual concentration can be done by comparison against a standard sample of known concentration with its EPR spectrum taken under identical conditions to that of the unknown. Knowing the concentration enables one, for instance, to obtain the dissociation constant of a paramagnetic ligand, for instance. As an example, Schiemann et al. used EPR to determine the binding number and dissociation constants of transition metal ligands (Mn^{2+}) to different ribozymes (44-46).

Mobility and dynamics

The mobility and dynamics of biomolecules can be effectively probed by EPR. When the molecule is frozen, the anisotropy of magnetic parameters such as g, hyperfine coupling (A) and electron-electron coupling (J, present in systems with multiple spin centers) influence the EPR spectrum the most (see Understanding Basic Spectra above). If the motion is very fast compared to the energy differences of these interactions, the anisotropies are washed out and the isotropic components of these interactions manifest themselves in a scalar fashion (as a number rather than as a tensor). In between these two extremes, the spectra are partially affected by the anisotropy, depending on the extent of the mobility of the spin centers. Spectra in Figure 2 show the effect of the mobility of a nitroxide spin label. Local dynamics of side chains and backbones of proteins, motion of lipids in biomembranes and the mobility of nucleic acids and saccharides can be investigated this way (47-51). Local and global rotational events can be distinguished by employing the frequency dependence of EPR resolution of motions differing in rate/speed (52).

pH

The local pH value plays a crucial role in biochemical reactions and thus the function of biological systems. The protonation state of amino acids and cofactors can be directly determined by EPR (7, 53). Non-invasive

local pH measurement *in vitro* and *in vivo* is also possible through *cw* EPR (54). For this purpose, either a carbon or a hydrogen atom of spin labels are substituted with an amino group thereby making them pH sensitive. Typically, the ring position 3 of the five-membered and the ring position 4 of the six-membered nitroxide spin labels are substituted. The spin density shift from the nitroxide nitrogen to the oxygen atom upon the protonation results in a reduced ^{14}N hyperfine coupling and an increased *g* value, which are easily measured by EPR. Most commonly, five-membered imidazolidine and imidazoline based nitroxides are used but non-nitroxide pH probes are also available (55, 56). The resolution of *g* anisotropy is not critical; therefore, the lower microwave frequencies can be used to turn the focus on the changes in hyperfine couplings. The use of lower microwave frequencies is particularly advantageous for *in vivo* measurements because their larger resonators/cavities allow use of larger samples (see also the section on instrumentation below) (57).

Taking one or two steps further

So far, we focused on the most basic *cw* EPR instrumentation, a spectrometer capable of acquiring a field sweep EPR signal at X-band (9.8 GHz/ 0.35mT). The resulting spectrum, however, is only one piece of the repertoire of EPR spectroscopy and one should not expect to get the whole story by a single spectrum. A couple of more pieces that may complete the job are introduced below.

cw ENDOR

While analyzing a *cw* EPR spectrum, small hyperfine couplings can be smaller than the linewidth and stay unresolved. Another obstacle in some cases is the large number of peaks; for a simple case on an isotropic spectrum with $S = ½$ and *n* equivalent protons ($I = ½$), $2n+1$ peaks are expected, each split by the isotropic hyperfine constant of *a* (aka A_{iso}). This number drastically changes, to 2^n, when the *n* protons are unequivalent and grows further if the spectrum is anisotropic (e.g. the sample is frozen). Electron Nuclear DOuble Resonance (ENDOR) offers a more direct detection of the electron-nuclear couplings and thus simplifies the determination of the hyperfine constants/tensors and the assignment of the spectral peaks. For the same two isotropic scenarios mentioned above, only 2 and $2n$ ENDOR peaks are expected, with the splitting between the corresponding pair of peaks being the hyperfine coupling constant (in frequency units; for an ENDOR energy scheme see Figure 2 in supplements). Figure 4 shows how the 28 line *cw* spectrum of phenalenyl radical, which has two classes of protons with a 6:3 ratio, "collapses" down to a 4 peak *cw* ENDOR spectrum from which the hyperfine coupling constants can be easily extracted (58). In practice, ENDOR is not quantitative and the spectrum is not symmetric (59). Furthermore, if hyperfine couplings are from different types of nuclei, ENDOR can help assign them to specific nuclei since the values of nuclear Larmor frequencies are detected directly alongside each hyperfine coupling. Nowadays, *cw* ENDOR is less frequently used due to the popularity of *pulsed* ENDOR; nevertheless, it shares the power of determining small and large hyperfine couplings. Note that additional hardware such as a radio frequency (RF) source, an RF amplifier, RF-coil-equipped resonator, etc. are necessary to perform ENDOR.

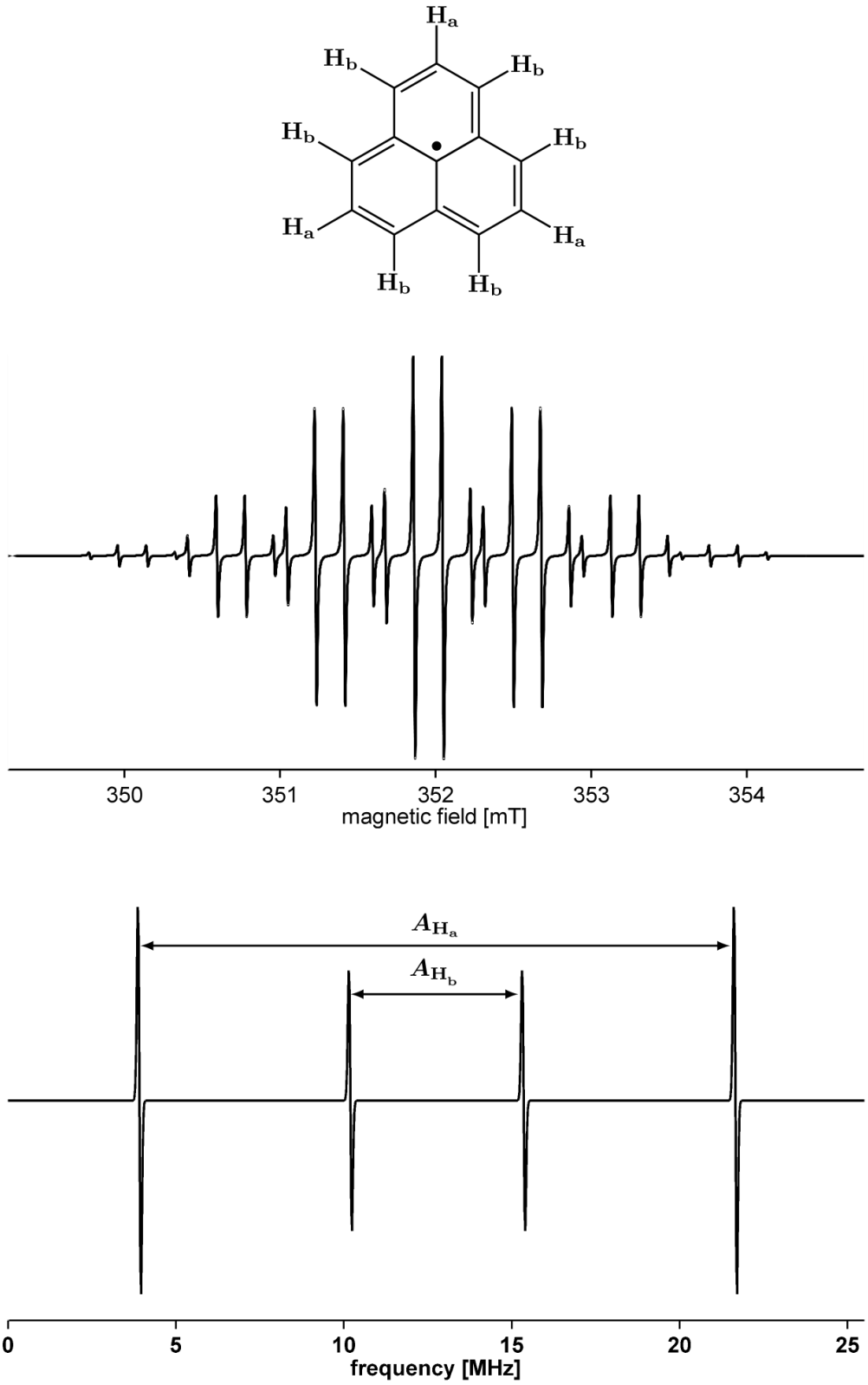

Figure 4. Simulated *cw* EPR and *cw*ENDOR spectra of phenalenyl radical. 28 peaks of the EPR spectrum are reduced to only 4 on the ENDOR spectrum, which is easier to interpret and relate to the hyperfine couplings. However, ENDOR is not a quantitative method, and in reality, it is not even symmetric most of the time.

Multi-frequency EPR

Usually, the determination of the *g* tensor and the hyperfine couplings (*A* tensors) are top priority when interpreting a field-sweep spectrum. However if, for instance, one considers the simple case of a spectrum with only two peaks, these two could stem from either a hyperfine coupling (splitting) or an isotropic *g* (or similarly two *g* values in the case of an isotropic experiment). The ambiguity is removed if a spectrum at a different frequency (and thus a different resonance magnetic field) is acquired. From the first two terms of the Hamiltonian expression in section "Understanding Basic Spectra", one notices that the electronic Zeeman term is field dependent while the hyperfine term is invariant, i.e. it is not affected by changes in the external field. This means that upon going to a higher frequency, the distance (in field units) between two peaks originating from two g components/ values increases while the hyperfine splittings (in field units) remain the same. Figure 5 shows the effect of the application of different microwave bands (frequencies) on the resolution of the anisotropy of *g* and *A* tensors.

Instrumentation

Common microwave bands which are used for EPR are L-, S-, X-, Q-, and W-bands, corresponding to the frequencies of ca. 1.1, 3.0, 9.7, 34 and 94 GHz, respectively (Fig. 5). The benefit and/or necessity of performing EPR at higher frequencies for obtaining higher resolution of *g* was discussed before. On the other hand, the dimensions of the resonators, which accommodate the sample and determine its maximum volume/size, is in the order of the wavelength of the applied microwave. This makes higher frequency EPR less sample-demanding while lower frequencies are advantageous in studying intrinsically large specimens such as living

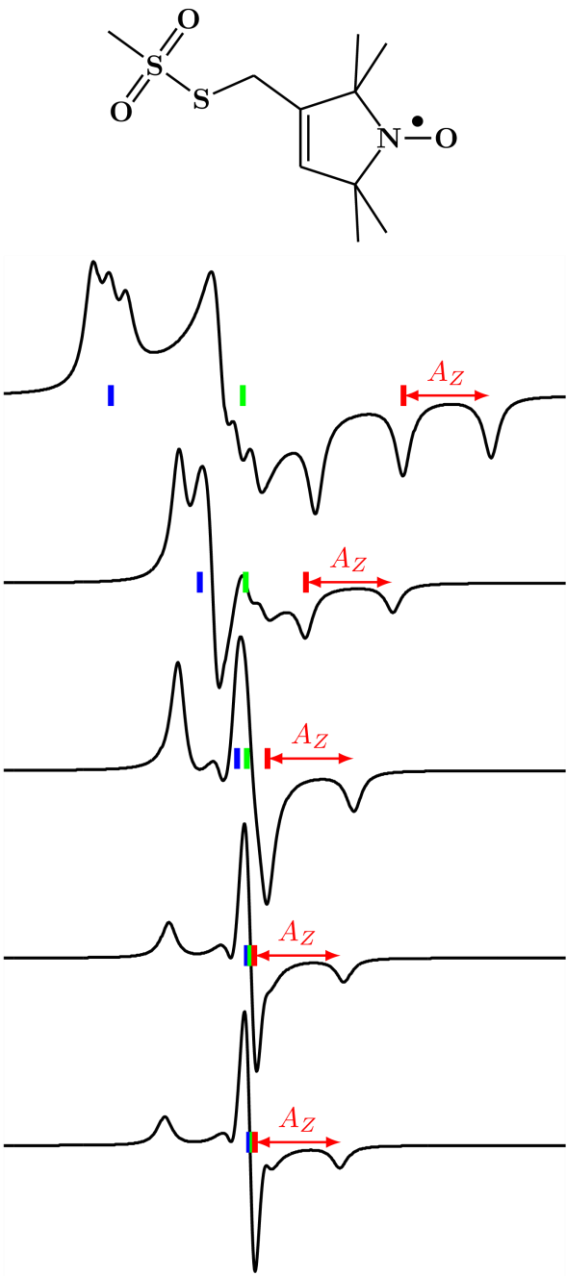

Figure 5. Simulated spectra of a typical nitroxide spin label at different microwave frequencies demonstrate the change in the resolution of the *g* tensor. The blue, green and red bars indicate g_x, g_y and g_z, the three principal values of the *g*, respectively. The abscissae represent the magnetic fields; they are shifted to include all the spectra on the same window for visual comparison, but they are on the same scale. While the *g* values become more and more resolved with higher frequencies, the hyperfine values and their corresponding splitting stay the same. From three principal values of hyperfine tensor *A*, the magnitude of the *z* component only, A_Z, is indicated with an arrow (3.8mT). The used frequencies correspond to L-, S-, X- Q- and W- microwave bands. See text for more details.

mice (60-62)! Traditionally, a lot of the EPR spectrometers are homebuilt and the development of special purpose and high frequency instruments is still common (63-65). The commercial providers are also pushing for new products, particularly instruments for higher frequencies. For instance, the availability of W-band (ca. 94 GHz) spectrometers by *Bruker BioSpin* made this frequency "conventional" and *Bruker* is now releasing the first commercial very high frequency EPR spectrometer at 263 GHz. Other suppliers of EPR spectrometers are *JEOL RESONANCE* and *magnettech*. Bench-top spectrometers with limited capabilities are also available from *Active Spectrum Inc.* and *ADANI*. Unfortunately, EPR is an expensive technique both at the level of initial instrumentation startup and at the level of consumables which include high quality quartz sample tubes and liquid helium for cooling the samples. But as discussed throughout this manuscript, the price is an investment towards valuable results.

Conclusion

Electron paramagnetic resonance spectroscopy (EPR) has shown its strength, versatility and multi-purpose nature in tackling biologically relevant questions and it can target any biological molecule, either with or without modifications. Unfortunately, its power surpasses its fame and EPR remains anonymous in some biological circles. This review was an effort to introduce biologists with little prior knowledge of EPR to this biophysical method and to highlight some of the main domains of application of *continuous wave* EPR for biomolecules.

Acknowledgements

The authors gratefully acknowledge support from the Deutsche Forschungsgemeinschaft for funding of this work within the SFB813 (Z1).

REFERENCES

1. Bairoch, A. (2000) The ENZYME database in 2000. *Nucleic Acids Research*, 28, 304-305.
2. Lu, Y., Yeung, N., Sieracki, N. and Marshall, N.M. (2009) Design of functional metalloproteins. *Nature*, 460, 855-862.
3. Kennedy, M.L. and Gibney, B.R. (2001) Metalloprotein and redox protein design. *Current Opinion in Structural Biology*, 11, 485-490.
4. Minnihan, E.C., Nocera, D.G. and Stubbe, J. (2013) Reversible, long-range radical transfer in E. coli class Ia ribonucleotide reductase. *Accounts of Chemical Research*, 46, 2524-2535.
5. Lovett, J.E., Bowen, A.M., Timmel, C.R., Jones, M.W., Dilworth, J.R., Caprotti, D., Bell, S.G., Wong, L.L. and Harmer, J. (2009) Structural information from orientationally selective DEER spectroscopy. *Physical Chemistry Chemical Physics*, 11, 6840-6848.
6. Tu, C.Q., Osborne, E.A. and Louie, A.Y. (2011) Activatable T (1) and T (2) magnetic resonance imaging contrast agents. *Ann. Biomed. Eng.*, 39, 1335-1348.
7. Stoll, S., NejatyJahromy, Y., Woodward, J.J., Ozarowski, A., Marletta, M.A. and Britt, R.D. (2010) Nitric oxide synthase stabilizes the tetrahydrobiopterin cofactor radical by controlling its protonation state. *Journal of the American Chemical Society*, 132, 11812-11823.
8. Gopalakrishnan, B., Nash, K.M., Velayutham, M. and Villamena, F.A. (2012) Detection of nitric oxide and superoxide radical anion by electron paramagnetic resonance spectroscopy from cells using spin traps. *Journal of visualized experiments : JoVE*, in press., e2810.
9. Kunjir, N.C., Reginsson, G.W., Schiemann, O. and Sigurdsson, S.T. (2013) Measurements of short distances between trityl spin labels with CW EPR, DQC and PELDOR. *Physical Chemistry Chemical Physics*, 15, 19673-19685.
10. Aziz, A., Hess, J.F., Budamagunta, M.S., Voss, J.C. and FitzGerald, P.G. (2010) Site-directed spin labeling and electron paramagnetic resonance determination of vimentin head domain structure. *Journal of Biological Chemistry*, 285, 15278-15285.
11. Engels, J., Grünewald, C. and Wicke, L. (2014) *In Chemical Biology of Nucleic Acids*. Erdmann, V.A., Markiewicz, W.T. and Barciszewski, J. (eds.), Springer Berlin Heidelberg, in press., 385-407.
12. Bordignon, E. and Polyhach, Y. (2013) In *Lipid-Protein Interactions*. Kleinschmidt, J.H. (ed.), Humana Press, Vol. 974, 329-355.
13. Fleissner, M.R., Brustad, E.M., Kálai, T., Altenbach, C., Cascio, D., Peters, F.B., Hideg, K., Peuker, S., Schultz, P.G. and Hubbell, W.L. (2009) Site-directed spin labeling of a genetically encoded unnatural amino acid. *Proceedings of the National Academy of Sciences*, 106, 21637-21642.
14. Reginsson, G.W., Shelke, S.A., Rouillon, C., White, M.F., Sigurdsson, S.T. and Schiemann, O. (2013) Protein-induced changes in DNA structure and dynamics observed with noncovalent site-directed spin labeling and PELDOR. *Nucleic Acids Research*, 41, e11.
15. Hagelueken, G., Abdullin, D., Ward, R. and Schiemann, O. (2013) mtsslSuite: In silico spin labelling, trilateration and distance-constrained rigid body docking in PyMOL. *Molecular Physics*, 111, 2757-2766.

16. Koto, T., Michalski, R., Zielonka, J., Joseph, J. and Kalyanaraman, B. (2014) Detection and identification of oxidants formed during •NO/O2•– reaction: A multi-well plate CW-EPR spectroscopy combined with HPLC analyses. *Free Radical Research*, 48, 478-486.

17. Barriga-Gonzalez, G., Aguilera-Venegas, B., Folch-Cano, C., Perez-Cruz, F. and Olea-Azar, C. (2013) Electron spin resonance as a powerful tool for studying antioxidants and radicals. *Current Medicinal Chemistry*, 20, 4731-4743.

18. Finkelstein, E., Rosen, G.M. and Rauckman, E.J. (1980) Spin trapping of superoxide and hydroxyl radical: Practical aspects. *Archives of Biochemistry and Biophysics*, 200, 1-16.

19. Dikalov, S.I. and Harrison, D.G. (2014) Methods for detection of mitochondrial and cellular reactive oxygen species. *Antioxid. Redox Signal.*, 20, 372-382.

20. Dikalov, S., Kirilyuk, I. and Grigor'ev, I. (1996) Spin trapping of O-, C-, and S-centered radicals and peroxynitrite by 2H-imidazole-1-oxides. *Biochemical and Biophysical Research Communications*, 218, 616-622.

21. Buettner, G.R. (1987) Spin trapping - electron-spin-resonance parameters of spin adducts. *Free Radic. Biol. Med.*, 3, 259-303.

22. Pievo, R., Angerstein, B., Fielding, A.J., Koch, C., Feussner, I. and Bennati, M. (2013) A rapid freeze-quench setup for multi-frequency EPR spectroscopy of enzymatic reactions. *ChemPhysChem*, 14, 4094-4101.

23. Kaufmann, R., Yadid, I. and Goldfarb, D. (2013) A novel microfluidic rapid freeze-quench device for trapping reactions intermediates for high field EPR analysis. *Journal of Magnetic Resonance*, 230, 220-226.

24. Kuchenreuther, J.M., Myers, W.K., Stich, T.A., George, S.J., NejatyJahromy, Y., Swartz, J.R. and Britt, R.D. (2013) A radical intermediate in tyrosine scission to the CO and CN− ligands of FeFe hydrogenase. *Science*, 342, 472-475.

25. Ryle, M.J., Lee, H. I., Seefeldt, L.C. and Hoffman, B.M. (2000) Nitrogenase reduction of carbon disulfide: freeze-quench EPR and ENDOR evidence for three sequential intermediates with cluster-bound carbon moieties†. *Biochemistry*, 39, 1114-1119.

26. Brunel, A., Santolini, J. and Dorlet, P. (2012) Electron paramagnetic resonance characterization of tetrahydrobiopterin radical formation in bacterial nitric oxide synthase compared to mammalian nitric oxide synthase. *Biophysical Journal*, 103, 109-117.

27. Stoll, S. and Schweiger, A. (2006) EasySpin, a comprehensive software package for spectral simulation and analysis in EPR. *Journal of Magnetic Resonance*, 178, 42-55.

28. Hanson, G.R., Gates, K.E., Noble, C.J., Griffin, M., Mitchell, A. and Benson, S. (2004) XSophe-Sophe-XeprView (R). A computer simulation software suite (v. 1.1.3) for the analysis of continuous wave EPR spectra. *J. Inorg. Biochem.*, 98, 903-916.

29. Eloranta, J. and Vuolle, M. (1998) Temperature dependence of the isotropic hyperfine coupling constants in 1,4-hydroquinone and 1,4-dihydroxynaphthalene cation radicals. *Magn. Reson. Chem.*, 36, 98-103.

30. Mombourquette, M.J. and Weil, J.A. (1992) Simulation of magnetic-resonance powder spectra. *Journal of Magnetic Resonance*, 99, 37-44.

31. Neese, F. (2012) The ORCA program system. *Wiley Interdiscip. Rev. Comput. Mol. Sci.*, 2, 73-78.

32. Zänker, P.P., Jeschke, G. and Goldfarb, D. (2005) Distance measurements between paramagnetic centers and a planar object by matrix Mims electron nuclear double resonance. *The Journal of Chemical Physics*, 122.

33. Moons, H., Łapok, Ł., Loas, A., Van Doorslaer, S. and Gorun, S.M. (2010) Synthesis, X-ray structure, magnetic resonance, and DFT analysis of a soluble copper(II) phthalocyanine lacking C−H bonds†. *Inorganic Chemistry*, 49, 8779-8789.

34. Huang, Y. W. and Chiang, Y. W. (2011) Spin-label ESR with nanochannels to improve the study of backbone dynamics and structural conformations of polypeptides. *Physical Chemistry Chemical Physics*, 13, 17521-17531.

35. Wegener, A.A., Klare, J.P., Engelhard, M. and Steinhoff, H.J. (2001) Structural insights into the early steps of receptor—transducer signal transfer in archaeal phototaxis. *The EMBO Journal*, 20, 5312-5319.

36. Hustedt, E.J. and Beth, A.H. (1999) Nitroxide spin-spin interactions: Applications to protein structure and dynamics. *Annu. Rev. Biophys. Biomolec. Struct.*, 28, 129-153.

37. Steinhoff, H.J., Radzwill, N., Thevis, W., Lenz, V., Brandenburg, D., Antson, A., Dodson, G. and Wollmer, A. (1997) Determination of interspin distances between spin labels attached to insulin: comparison of electron paramagnetic resonance data with the X-ray structure. *Biophysical Journal*, 73, 3287-3298.

38. Rabenstein, M.D. and Shin, Y.K. (1995) Determination of the distance between two spin labels attached to a macromolecule. *Proceedings of the National Academy of Sciences*, 92, 8239-8243.

39. Marsh, D. (2014) Intermediate dipolar distances from spin labels. *Journal of Magnetic Resonance*, 238, 77-81.

40. Hustedt, E.J., Smirnov, A.I., Laub, C.F., Cobb, C.E. and Beth, A.H. (1997) Molecular distances from dipolar coupled spin-labels: the global analysis of multifrequency continuous wave electron paramagnetic resonance data. *Biophysical Journal*, 72, 1861-1877.

41. Banham, J.E., Baker, C.M., Ceola, S., Day, I.J., Grant, G.H., Groenen, E.J.J., Rodgers, C.T., Jeschke, G. and Timmel, C.R. (2008) Distance measurements in the borderline region of applicability of CW EPR and DEER: A model study on a homologous series of spin-labelled peptides. *Journal of Magnetic Resonance*, 191, 202-218.

42. Borbat, P. and Freed, J. (2013) In *Structural Information from Spin-Labels and Intrinsic Paramagnetic Centres in the Biosciences*. Timmel, C.R. and Harmer, J.R. (eds.), Springer Berlin Heidelberg, Vol. 152, 1-82.

43. Fee, J.A. (1978) *In Methods in Enzymology*. C.H.W. Hirs, S.N.T. (ed.), Academic Press, Vol. 49, 512-528.

44. Kisseleva, N., Khvorova, A., Westhof, E. and Schiemann, O. (2005) Binding of manganese(II) to a tertiary stabilized hammerhead ribozyme as studied by electron paramagnetic resonance spectroscopy. *RNA*, 11, 1-6.

45. Kisseleva, N., Kraut, S., Jäschke, A. and Schiemann, O. (2007) Characterizing multiple metal ion binding sites within a ribozyme by cadmium-induced EPR silencing. *HFSP Journal*, 1, 127-136.

46. Kisseleva, N., Khvorova, A., Westhof, E., Schiemann, O. and Wolfson, A.D. (2008) The different role of high-affinity and low-affinity metal ions in cleavage by a tertiary stabilized cis hammerhead ribozyme from tobacco ringspot virus. *Oligonucleotides*, 18, 101-110.

47. Hubbell, W.L. and Altenbach, C. (1994) Investigation of structure and dynamics in membrane proteins using site-directed spin labeling. *Current Opinion in Structural Biology*, 4, 566-573.

48. Columbus, L. and Hubbell, W.L. (2002) A new spin on protein dynamics. *Trends in Biochemical Sciences*, 27, 288-295.

49. Weber, S., Wolff, T. and Bünau, G.v. (1996) Molecular mobility in liquid and in frozen micellar solutions: EPR spectroscopy of nitroxide free radicals. *Journal of Colloid and Interface Science*, 184, 163-169.

50. Nguyen, P. and Qin, P.Z. (2012) RNA dynamics: perspectives from spin labels. *Wiley Interdisciplinary Reviews: RNA*, 3, 62-72.

51. Malferrari, M., Nalepa, A., Venturoli, G., Francia, F., Lubitz, W., Mobius, K. and Savitsky, A. (2014) Structural and dynamical characteristics of trehalose and sucrose matrices at different hydration levels as probed by FTIR and high-field EPR. *Physical Chemistry Chemical Physics*, 16, 9831-9848.

52. Nesmelov, Y. and Thomas, D. (2010) Protein structural dynamics revealed by site-directed spin labeling and multifrequency EPR. *Biophys Rev*, 2, 91-99.

53. Mino, H., Kawamori, A. and Ono, T.A. (2000) pH-dependent characteristics of YZ radical in Ca^{2+}-depleted Photosystem II studied by CW-EPR and pulsed ENDOR. *Biochimica et Biophysica Acta (BBA) - Bioenergetics*, 1457, 157-165.

54. Khramtsov, V.V., Grigor'ev, I.A., Foster, M.A. and Lurie, D.J. (2004) In vitro and in vivo measurement of pH and thiols by EPR-based techniques. *Antioxid. Redox Signal.*, 6, 667-676.

55. Liu, Y., Villamena, F.A. and Zweier, J.L. (2008) Highly stable dendritic trityl radicals as oxygen and pH probe. *Chemical Communications*, in press., 4336-4338.

56. Bobko, A.A., Dhimitruka, I., Komarov, D.A. and Khramtsov, V.V. (2012) Dual-function pH and oxygen phosphonated trityl probe. *Analytical Chemistry*, 84, 6054-6060.

57. Gallez, B., Mader, K. and Swartz, H.M. (1996) Noninvasive measurement of the pH inside the gut by using pH-sensitive nitroxides. An in vivo EPR study. *Magnetic Resonance in Medicine*, 36, 694-697.

58. Murphy, D.M. and Farley, R.D. (2006) Principles and applications of ENDOR spectroscopy for structure determination in solution and disordered matrices. *Chemical Society Reviews*, 35, 249-268.

59. Kulik, L. and Lubitz, W. (2009) Electron-nuclear double resonance. *Photosynth Res*, 102, 391-401.

60. Sotgiu, A., Mader, K., Placidi, G., Colacicchi, S., Ursini, C.L. and Alecci, M. (1998) pH-sensitive imaging by low-frequency EPR: a model study for biological applications. *Phys. Med. Biol.*, 43, 1921-1930.

61. Komarov, A. (2002) In vivo detection of nitric oxide distribution in mice. *Mol Cell Biochem*, 234-235, 387-392.

62. Swartz, H.M., Khan, N. and Khramtsov, V.V. (2007) Use of electron paramagnetic resonance spectroscopy to evaluate the redox state in vivo. *Antioxid. Redox Signal.*, 9, 1757-1771.

63. Yokoyama, H. (2012) Direct EPR irradiation of a sample using a quartz oscillator operating at 250 MHz for EPR measurements. *Journal of Magnetic Resonance*, 214, 119-123.

64. Dutka, M., Oles, T., Mossakowski, M. and Froncisz, W. (2011) Rectangular loop-gap resonator with the light access to the sample. *Journal of Magnetic Resonance*, 210, 44-50.

65. Reijerse, E., Lendzian, F., Isaacson, R. and Lubitz, W. (2012) A tunable general purpose Q-band resonator for CW and pulse EPR/ENDOR experiments with large sample access and optical excitation. *Journal of Magnetic Resonance*, 214, 237-243.